34th Annual International Conference of the IEEE EMBS
San Diego, California USA, 28 August - 1 September, 2012

Support of a patient–specific therapeutical acoustic stimulation in tinnitus by numerical modeling

Haab, L.[1], Scheerer, M.[1], Ruckert, J.[1], Hannemann, R.[4], and Strauss, D.J.[1,2,3]

Abstract—**The pathogenesis of tinnitus involves multiple hierarchical levels of auditory processing and appraisal of sensory saliency. Early tinnitus onset is most likely attributed to homeostatic plasticity in the periphery, while the chronification and decompensation are tightly linked to brain areas for the allocation of attentional resources, such as e.g., the thalamocortical feedback loops and the limbic system. Increased spontaneous firing after sensory deafferentation might be sufficient to generate a phantom perception, yet the question why not every peripheral hearing loss automatically elicits a tinnitus sensation is still to be addressed. Utilizing quantitative modeling of multiple hierarchical levels in the auditory pathway, we demonstrate the effects of lateral inhibition on increased spontaneous firing and the resulting elevation of firing regularity and synchronization of neural activity. The presented therapeutical approach is based on the idea of disrupting the heightened regularity of the neural population response in the tinnitus frequency range. This neural activity regularity depends on lateral dispersion of common noise and thus is susceptible for edge effects and might be influenced by a change in neural activity in bordering frequency ranges by fitted acoustical stimulation. We propose the use of patient specifically adapted tailor-made notched acoustic stimulation, utilizing modeling results for the optimal adjustment of the stimulation frequencies to archive a therapeutical edge–effect.**

I. INTRODUCTION

In the majority of cases tinnitus is associated with a peripheral high–frequency hearing loss. The population of high–risk–groups for hearing loss due to noise exposure or age, thus also has a higher prevalence for tinnitus [1]. Tinnitus can also occur in normal hearing subjects, but is in most of these cases characterized by a significantly lower degree of severity compared to tinnitus sufferers with hearing loss [2]. A recent study by Schaette et al. [3] demonstrates a reduced amplitude of the *wave I* potential in brainstem audiometry in tinnitus sufferers with a normal audiogram. This reduction hints towards a "hidden hearing loss" and peripheral origin of the tinnitus as the neural response magnitude is renormalized within subsequent processing stages. Experimental support for this hypothesis was presented by Weisz et al [4]. This phenomenon of phantom perceptions related to peripheral deafferentation is not strictly related to the auditory pathway, but appears also in a number of comparable symptomatologies as phantom (limb) pain (PP) [5] or Charles Bonnet (CB) syndrome due to macular degeneration [6]. All these symptomatologies have in common a hyperactivity / hyperexcitability of the deafferentated midbrain neurons, demonstrated, e.g., by increased metabolism rate [7], [8] (CB),[9] (PP). Mulders et al. recently presented experimental results on the relationship between hair cell loss, auditory thresholds and spontaneous activity in the central nucleus of the inferior colliculus (CNIC) in guinea pigs [10] related to frequency bands with peripheral hearing loss after acoustic trauma. The authors could assess an increase of spontaneous neural activity in the CNIC in frequencies less than one octave in distance to the frequency of the acoustic trauma with a maximum near or slightly above the exposure frequency. The persistent spontaneous firing frequency of CNIC neurons in the tonotopic range of the noise exposure frequency increased significantly in animals with severe acoustic trauma [10]. The increase of the spontaneous firing rate can be considered as a physiological compensation process in response to a notch like hearing loss and the related deafferentation of higher levels of sensory processing.

This phenomenon is yet not sufficient to explain why and how the tinnitus percept arises and the mechanisms of tinnitus decompensation. Also the discrepancy of subjectively perceived tinnitus loudness and objective loudness masking measures is not explicable on the base of the increased spontaneous firing rate alone. Studies in non–linear dynamics demonstrated a phase synchronization of limit–cycle oscillators, e.g., Hodgkin–Huxley oscillators, subject to common impulse noise input [11], [12]. As the cortex is driven by weak but synchronously active thalamocortical synapses [13] the probability of generating a percept as result of higher–order spiking correlation in a population of thalamocortical neurons increases with the firing rate [14]. The increased spiking coherence must thus be seen as base for synchronous activity across a neural population, which might be sufficient to activate higher processing stages. Attentional top–down mechanisms further boost the synchronous activity of thalamocortical neuron populations in the sensory pathway [15], improving the competitive advantage of the stimulus in perceptual rivalry [16], [17] which might consequently lead to a consolidation of information processing during the chronification process.

Pantev et al demonstrated the therapeutical effect of tailor–made notched acoustical stimulation (TMNAS) in tinnitus sufferers [18]. After one year of TMNAS therapy, the patient group reported reduced subjective tinnitus distress accompanied with reduced evoked activity in auditory cortex compared to a placebo treated reference group. The authors attribute the improvement of subjective tinnitus loudness to induced cortical reorganization by lateral inhibition [19] and

[1]L. Haab, M. Scheerer, J. Ruckert and D.J. Strauss are with Systems Neuroscience Neurotechnology Unit, Neurocenter, Saarland University Hospital, Homburg/Saar, Germany haab@snn-unit.de

[2]D.J. Strauss is also with INM - Leibniz Institute for New Materials, Saarbrücken, Germany strauss@snn-unit.de

[3]D.J. Strauss is also with Key Numerics, Saarbrücken, Germany

[4]R. Hannemann is with Siemens Audiologische Technik, Erlangen, Germany

activation of the brain's reward system as result of pleasant acoustic stimulation [20]. As the cortical effects of acoustic stimulation in the TMNAS therapy are already analyzed in detail, we focused in this article on the simulation of subthalamic effects of increased compound action potentials and lateral inhibition, providing additional support or the use of tailor–made notched acoustic stimulation as support in the tinnitus intervention.

II. Materials and Methods

For modeling purposes we can describe the spontaneous activity of a nerve by a Poisson point process, in which each point represents a spike, due to the fact that no actual information is conveyed by the shape of the action potential [21].

A. Modeling homeostatic plasticity

The increase in spontaneous neural activity in the periphery of the auditory pathway can be attributed to homeostatic plasticity. Schaette et al [22] presented a quantitative model for simulating the elevated neural response due to peripheral deafferentation. The averaged population firing rate f for a given stimulus intensity I of the auditory nerve (AN) in healthy condition can be described by

$$f(I) = \begin{cases} f_{sp} & \text{for} \quad I < I_\theta \\ f_{sp} + (f_{max} - f_{sp}) \frac{\int_{I_\theta}^{I} p(I)dI}{1 - p_{sp}} & \text{for} \quad I > I_\theta \end{cases} \tag{1}$$

where f_{sp} is the spontaneous neural activity, $p(I)$ is the probability density distribution of the stimulus intensity level I. f_{max} denotes the maximum discharge rate of the neural population. I_θ is a threshold–intensity [22], [23].

The threshold of AN fibers θ increases proportional to a loss of outer hair cells or stereocilia, leading to a elevated probability of spontaneous firing and reduced stimulus driven activity. A downstream neuron receives spontaneous input from AN with rate f_{sp} and from other sources f_{add}. The spontaneous firing rate r_{sp} of this downstream neuron is given by

$$r_{sp} = r_{high} \; tanh\left(\frac{g(f_{sp} + f_{add}) - \theta}{r_{high}}\right) \quad \text{for} \quad g(f_{sp} + f_{add}) > \theta \tag{2}$$

in which the slope steepness depends on a gain factor g and the summed activity of the preceding neuron and additional sources compared to a threshold value θ. The mean firing rate of the neural population $\bar{r}$ is calculated by

$$\bar{r} = \int_{r_{sp}}^{r_{max}} r \; q(r) \; dr \tag{3}$$

in which $q(r)$ denotes the probability density distribution of the models firing rate. r_{sp} and r_{max} depend on g so that $\bar{r}$ increases with increasing g. The aforementioned effects result in a decrease of the mean firing rate due to an overrepresentation of spontaneous activity. If the mean firing rate $\bar{r}$ does not match a preset value $\overline{r^*}$, homeostatic plasticity takes places to restore the mean firing rate by increasing the gain factor g, amplifying also the spontaneous neural activity rate.

B. Dorsal cochlear nucleus (DCN) numerical model

The DCN model is based on the neuromime model by MacGregor et al [24] and the implementation by Zheng et al. [25] The membrane potential V_{mem} in this single–compartment model is influenced by variable gating parameters g_K, g_{ex}, and g_{in}, denoting potassium, excitatory, and inhibitory conductances. It is

$$\tau_{mem} \frac{dV_{mem}}{dt} = -V_{mem} - g_K(V_{mem} - E_K) - g_{ex}(V_{mem} - E_{ex}) - g_{in}(V_{mem} - E_{in}) \tag{4}$$

$$\tau_K \frac{dg_k}{dt} = -g_K + b_K S \tag{5}$$

$$S = 1 \quad \text{if} \quad V_{mem} \geq \theta \tag{6}$$

where E_K, E_{ex}, and E_{in} are potassium, excitatory, and inhibitory reversal potentials. The parameter b_K influences the models sensitivity to potassium conductance and S indicates a generated action potential. The variable conductance g for the target cell, representing N converging synapses is given by

$$\tau \frac{dg}{dt} = -g + \sigma \sum_{i=1}^{N} S_i \tag{7}$$

where σ is the step conductance increase and and τ the response time constant to incoming spikes. S_i is a series of spikes derived from output of the antecedent processing stages. The DCN model accounts for three types of neurons. Please enquire [25] for a list of intrinsic neuron–type parameters. Figure 1 depicts the neural interconnection for a single patch of the DCN.

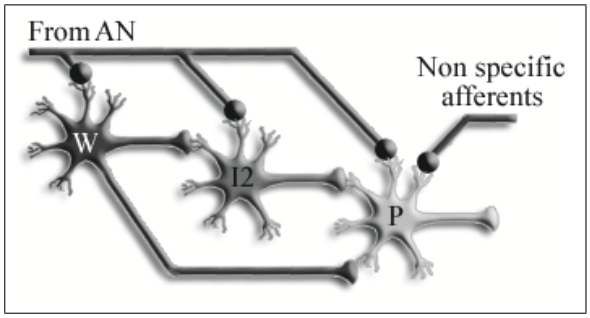

Fig. 1. Schematic representation of the DCN neural interconnections. Depicted are 3 types of DCN neurons: P(Type III/Type IV), I2(Type II), W(wideband inhibition). Ball shaped synapses are excitatory, cone shaped synapses are inhibitory. AN(Auditory Nerve).

C. Lateral inhibition network

For the lateral inhibition network of a Inferior Colliculus (IC) model we set up a lattice structure of 800 principal neurons, interconnected by inhibitory interneurons. The strength and width of lateral inhibition is given by a Gaussian distribution. The simulated network on which the effects of lateral inhibition and spontaneous hyperactivity were tested is

based on Izhikevich's simple spiking neuron model [26]. The intrinsic dynamics of the model follow the coupled differential equations

$$\begin{aligned} \frac{dv}{dt} &= 0.04v^2 + 5v + 140 - u + I_{input} \\ \frac{du}{dt} &= a(bv - u) \end{aligned} \tag{8}$$

with a reset condition:

$$\text{if } v(t) > 30mV, \quad \text{then } \begin{cases} v = c \\ u = u + d \end{cases} \tag{9}$$

The parameter v indicates the membrane potential, u is a recovery variable. I_{input} is the spike series output of the antecedent DCN model. The parameters *a, b, c*, and *d* were adjusted to match the neural properties of IC neurons. Parameter a alters the temporal scale of the recovery variable u, while parameter b regulates the sensitivity of u to subthreshold membrane fluctuations. The parameter c determines the after–spike reset potential; d alters the after–spike reset of u.

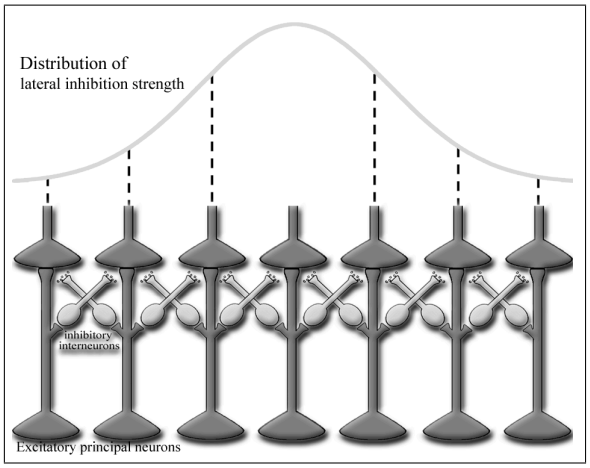

Fig. 2. Schematic representation of the lateral inhibition network and spatial attenuation of inhibition strength.

III. Results and Discussion

The increase of stimulus intensity and neural firing rate has a direct influence on the neural response reliability (RR). The coefficient of variation (CV), given by $\frac{1}{\sqrt{\lambda}}$ with λ denoting mean and variance of the underlying Poisson distribution, decreases with increasing spontaneous activity. In our simulation, we modeled the influence of elevated firing rates due to acoustical stimulation on neural RR. Lateral inhibition accounts for an increase of CV while the neural populations bordering the hearing notch respond to an acoustic stimulus. The reduction of RR might provide an auspicious base for early therapeutical intervention. Using a notched acoustical stimulation centering the tinnitus frequency the effect described above can be archived. See Pantev et al. for experimental results in *tailor–made notched–music* tinnitus therapy [18]. For further early therapeutical intervention we propose the use of patient–specifically adapted tailor-made notched acoustic

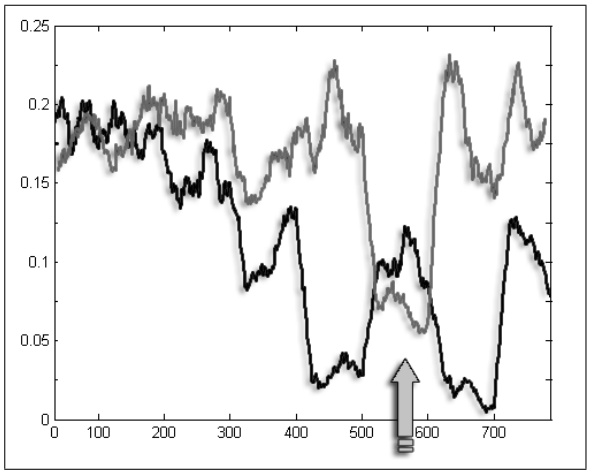

Fig. 3. Exemplary coefficient of variation over 800 artificial neurons in the lateral inhibition network model for spontaneous activity with increased firing rate due to homeostatic plasticity (grey line – arrow indicates neural population with elevated mean firing rate) and for stimulated activity with exaggerated neural response frequencies in regions bordering the simulated hearing impairment (black line).

stimulation, combined with psychological counseling. The auditory stimulator's frequency bands can be modified using a patient–specific notch filter centered on the individual tinnitus frequency. This approach allows for a reduction of neural RR and subsequent involuntary allocation of attentional resources in support of conventional tinnitus therapy and retraining. To minimize technical noise in the devices and for a limitation of the overall noise exposure, we only exaggerate the frequencies bordering the subjective tinnitus. The presented models of the subthalamic auditory system can serve as guideline for the patient–specific adaptation of these acoustic stimulation devices.

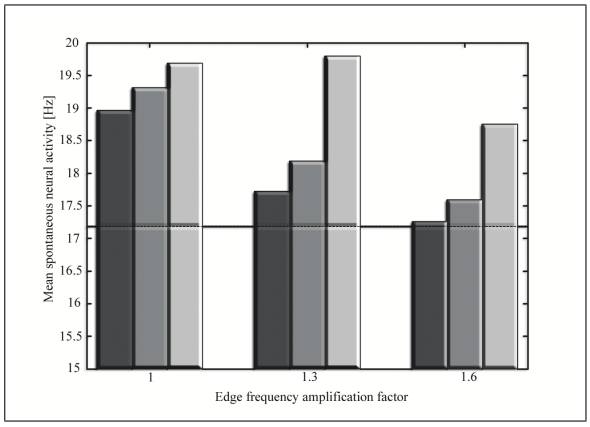

Fig. 4. Mean activity in tonotopic area of cochlear lesion after acoustical stimulation. Stimulus was notched with bandwidths of 1.4kHz (dark grey), 1.6kHz (medium grey) and 2kHz (light grey) centering the modeled tinnitus frequency. Level of spontaneous mean activity is indicated by dashed line. Left bars indicate pure stimulus without edge frequency amplification. For middle and right section the amplification factor for frequencies bordering the notch was 1.3 and 1.6 respectively.

In figure 4 and table I we show the effects of notched stimulation on simulated neural response rates in comparison

to mean spontaneous firing. The efficiency of notched stimulation on mean activity rates and firing reliability depends on the characteristics of the edge effect and thus from notch bandwidth and exaggeration of bordering frequencies. Ideally the pathologically increased spontaneous firing, resulting from homeostatic compensation processes in the tinnitus frequency can be reduced to the level of mean spontaneous activity in the physiological condition. For narrow notch bandwidth and moderate exaggeration of bordering frequencies, the simulated pathologic neural activity was reduced to an almost physiological state of spontaneous firing.

TABLE I
EXEMPLARY MEAN FIRING RATES AND STANDARD DEVIATIONS FOR NOTCHED STIMULATION WITH VARIABLE NOTCH BANDWIDTH AND EXAGGERATION OF FREQUENCIES BORDERING THE NOTCH; γ DENOTES AMPLIFICATION FACTOR. THE SIMULATED HEARING DEFICIT IS LOCATED AT 3KHZ

Notch bandwidth in kHz	$\gamma = 1$	$\gamma = 1.3$	$\gamma = 1.6$
1.4	18.96($\pm$0.96)	17.72($\pm$1.21)	17.26($\pm$1.34)
1.6	19.31($\pm$0.81)	18.18($\pm$0.94)	17.59($\pm$0.87)
2.0	19.68($\pm$0.95)	19.80($\pm$1.39)	18.75($\pm$0.94)

A. Limitations and future work

The spread of coherent information in the auditory pathway due to lateral inhibition is still a parameter in the proposed model that is hard to access in the individual tinnitus patient. The design of adaptable paradigms capitalizing, e.g., on the Zwicker tone illusion [27] or masking effects, is inevitable in the patient–specific adaptation of the therapeutical stimulators for tinnitus treatment and for future refinement of the proposed models. Although we can not reliably present absolute numbers for firing rates, the characteristic trend of neural behaviour becomes visible. Lateral inhibition in physiological condition is asymmetrical, generating a shift in the compound action potential of neighboring neuron populations [28]. Future work will involve refinement of the proposed rudimentary framework using animal–experimental data on the spread of lateral inhibition. The prospective high–resolution data allows for a detailed adjustment of the few free model parameters to physiological conditions.

REFERENCES

[1] H. Hoffman and G. Reed, *Tinnitus: theory and management*. Lewiston: BC Decker, 2004, ch. Epidemiology of tinnitus, pp. 16–41.

[2] M. Savastano, "Tinnitus with or without hearing loss: are its characteristics different?" *Eur Arch Otorhinolaryngol*, vol. 265, pp. 1295–1300, 2008.

[3] R. Schaette and D. McAlpine, "Tinnitus with a normal audiogram: physiological evidence for hidden hearing loss and computational model," *J Neurosci*, vol. 31, pp. 13 452–13 457, 2011.

[4] N. Weisz, T. Hartmann, K. Dohrmann, W. Schlee, and A. Norena, "High-frequency tinnitus without hearing loss does not mean absence of deafferentation," *Hear Res*, vol. 222, pp. 108–114, 2006.

[5] D. De Ridder, A. Elgoyhen, R. Romo, and B. Langguth, "Phantom percepts: tinnitus and pain as persisting aversive memory networks," *Proc Natl Acad Sci USA*, vol. 108, pp. 8075–8080, 2011.

[6] J. Jang, Y. Youn, J. Seok, S. Ha, H. Shin, S. Ahan, K. Park, and O. Kwon, "Hypermetabolism in the left thalamus and right inferior temporal area on positron emission tomography–statistical parametric mapping (pet-spm) in a patient with charles bonnet syndrome resolving after treatment with valproic acid," *J Clin Neurosci*, vol. 18, pp. 1130–1132, 2011.

[7] W. Burke, "The neural basis of charles bonnet hallucinations: a hypothesis," *J Neurol Neurosurg Psychiatry*, vol. 73, pp. 535–541, 2002.

[8] N. Adachi, T. Watanabe, H. Matsuda, and T. Onuma, "The neural basis of charles bonnet hallucinations: a hypothesis," *Psychiatry and Clinical Neurosciences*, vol. 54, pp. 157–162, 2000.

[9] H. Flor, "Phantom-limb pain: characteristics, causes, and treatment," *Lancet Neurol*, vol. 1, pp. 182–189, 2002.

[10] W. Mulders, D. Ding, R. Salvi, and D. Robertson, "Relationship between auditory thresholds, central spontaneous activity, and hair cell loss after acoustic trauma," *J Comp Neurol*, vol. 519, pp. 2637–2647, 2011.

[11] H. Nakao, K. Arai, K. Nagai, Y. Tsubo, and Y. Kuramoto, "Synchrony of limit-cycle oscillators induced by random external impulses," *Physical Review*, vol. 72, 2005.

[12] P. Danzl, R. Hansen, G. Bonnet, and J. Moehlis, "Partial phase synchronization of neural populations due to random poisson inputs," *J Comput Neurosci*, vol. 25, pp. 141–157, 2008.

[13] R. Bruno and B. Sakmann, "Cortex is driven by weak but synchronously active thalamocortical synapses," *Science*, vol. 312, pp. 1622–1627, 2006.

[14] S. Grun, M. Abeles, and M. Diesmann, *Dynamic Brain – from Neural Spikes to Behaviors*. Heidelberg: Springer Press, 2008, ch. Impact of higher–order correlations on coincidence distributions of massively parallel data, pp. 96–114.

[15] C. Trenado, L. Haab, and D. J. Strauss, "Multiscale modeling of auditory attention: Forward modeling of large–scale neural correlates in evoked potentials," *IEEE Trans Neural Syst Rehabil Eng.*, vol. 17, pp. 46–52, 2008.

[16] C. Börgers and N. Kopell, "Gamma oscillations and stimulus selection," *Neural Comput*, vol. 20, pp. 383–414, 2008.

[17] P. Fries, J. Schröder, P. Roelfsema, W. Singer, and A. Engel, "Oscillatory neuronal synchronization in primary visual cortex as a correlate of stimulus selection," *J. Neurosci*, vol. 22, pp. 3739–3754, 2002.

[18] H. Okamoto, H. Stracke, W. Stoll, and P. C., "Listening to tailor-made notched music reduces tinnitus loudness and tinnitus-related auditory cortex activity," *Proc Natl Acad Sci USA*, vol. 107, pp. 1207–1210, 2010.

[19] C. Pantev, H. Okamoto, B. Ross, W. Stoll, E. Ciurlia-Guy, R. Kakigi, and T. Kubo, "Lateral inhibition and habituation of the human auditory cortex," *Eur J Neurosci*, vol. 19, pp. 2337–2344, 2004.

[20] A. Blood and R. Zatorre, "Intensely pleasurable responses to music correlate with activity in brain regions implicated in reward and emotion," *Proc Natl Acad Sci USA*, vol. 98, pp. 11 818–11 823, 2001.

[21] D. Perkel, G. Gerstein, and G. Moore, "Neuronal spike trains and stochastic point processes," *Biophys J*, vol. 7, pp. 419–440, 1967.

[22] R. Schaette and R. Kempter, "Development of tinnitus-related neuronal hyperactivity through homeostatic plasticity after hearing loss: a computational model," *Eur J Neurosci*, vol. 23, pp. 3124–3138, 2006.

[23] S. Laughlin, "A simple coding procedure enhances a neurons information capacity," *Z. Naturforsch*, vol. 36, pp. 910–912, 1981.

[24] R. MacGregor, *Neural and brain modeling*. San Diego: Academic Press, 1987.

[25] X. Zheng and H. Voight, "Computational model of response maps in the dorsal cochlear nucleus," *Biol Cybern*, vol. 95, pp. 233–242, 2006.

[26] E. Izhikevich, "Simple model of spiking neurons," *IEEE Transactions on Neural Networks*, vol. 14, pp. 1569–1572, 2003.

[27] A. Norena, C. Micheyl, and S. Chery-Croze, "An auditory negative after-image as a human model of tinnitus," *Hear Res*, vol. 149, pp. 24–32, 2000.

[28] H. Okamoto, R. Kakigi, A. Gunji, and C. Pantev, "Asymmetric lateral inhibitory neural activity in the auditory system: a magnetoencephalographic study," *BMC Neurosci*, vol. 17, pp. 8–33, 2007.